Serpentine Superlattice Quantum-Wire Arrays of (Al,Ga)As Grown on Vicinal GaAs Substrates

M. S. Miller,[1] H. Weman,[2],[a] C. E. Pryor,[3] M. Krishnamurthy,[4] P. M. Petroff,[1],[4]
H. Kroemer,[1],[4] and J. L. Merz[1],[2]

[1]*Department of Electrical and Computer Engineering, University of California, Santa Barbara, California 93106*
[2]*Center for Quantized Electronic Structures, University of California, Santa Barbara, California 93106*
[3]*Physics Department, University of California, Santa Barbara, California 93106*
[4]*Engineering Materials Department, University of California, Santa Barbara, California 93106*

(Received 22 July 1991; revised manuscript received 7 February 1992)

A serpentine superlattice quantum-wire array avoids the tilt sensitivity of a tilted superlattice and promises significant 1D confinement at the 10 nm scale. Transmission electron micrographs confirm the intended geometry. Three independent polarization measurements, an energy shift, and the light-hole–heavy-hole splitting at 1.4 K, when compared with theory, demonstrate 1D valence band states and 2D conduction band states. All five measurements are explained by lateral $Al_xGa_{1-x}As$ wells and barriers of $x=0.12$ and 0.21, respectively, thus characterizing the step-flow growth.

PACS numbers: 73.20.Dx, 78.55.Cr, 78.65.Fa

Several approaches to quasi-one-dimensional (1D) semiconducting systems have been pursued [1–10]. Of principal interest is the energy scale of the 1D confinement, E_{1D}, which corresponds to the subband spacing and is set by the size l of the well, the effective mass, and the height of the confining potential V. The various "quantum-wire" techniques include patterning thin 2D layers for additional lateral confinement with electrostatic [1] or strain fields [2], and patterning a substrate for a subsequent epitaxial growth [3]. Laterally, V may be a few hundred meV for these systems, though l is limited by the lithography to the order of 100 nm, resulting in E_{1D} of 1 to 10 meV being reported. Cleaved InAs quantum-well (QW) structures that have a 1D electron gas electrostatically confined at the free QW edge [4] have been reported, as have attempts at epitaxial overgrowth on cleaved (Al,Ga)As heterostructure edges [5]. Both cleaving techniques can have $l\sim10$ nm and $V\sim100$ meV, which could give E_{1D} of several tens of meV. Recently, QWs have been reported directly grown on naturally microfaceted surfaces [6]. The resulting 1 nm high corrugations have a lateral period of $l\sim3$ nm, perturbing a ~5 nm QW, which is not enough for lateral confinement. The technique of this Letter is the epitaxial growth on atomically stepped, vicinal substrates, where arrays parallel to the step edges are formed by alternating between partial layers of different composition [7]. The lateral period, determined by the vicinal angle α and step height d, is on the order of $l\sim10$ nm, while V will depend on the degree of lateral composition modulation and could ideally be as high as several hundred meV, giving $E_{1D}\sim100$ meV. To date, confinement to 1D has not been established and reported for these systems.

Vicinal-substrate growths have been employed to form (Al,Ga)As [8] and (Al,Ga)Sb [9] "tilted superlattices" (TSLs) using molecular beam epitaxy (MBE), and (Al,Ga)As "fractional layer superlattices" using metalorganic chemical vapor deposition [10]. Some lateral composition modulation has been shown with transmission electron microscopy (TEM) [8,9] and x-ray diffraction [10]. Anisotropy has been reported in the polarized photoluminescence excitation (PLE) of a QW corrugated with a TSL [11]. Such behavior, though, is not expected for that structure [12] and the claimed anisotropy arose from experimental artifacts [13]. Similar anisotropy for a single-monolayer lateral superlattice inserted in the center of a QW has been reported [14], which is consistent with the prediction that even elongated AlAs islands in GaAs QWs should give anisotropy [15]. The lateral superlattices reported in Refs. [6,11,14] will *perturb* the QWs but not *confine* states to 1D. The optical anisotropy itself is not of interest, but rather the electronic structure from which it arises.

Central to preparing these epitaxial quantum wires are the current topics of the physics of surface diffusion [16], vicinal surfaces [17], and crystal growth mechanisms [18]. A step-flow growth mechanism is intended to dominate competing processes and give segregation to and incorporation into straight step edges. Reflection high-energy electron diffraction may be used during growth, though it does not provide detailed step structure or composition information [19]. Scanning tunneling microscopy [20] has revealed details of stepped vicinal surfaces and could in principle measure the composition, but cannot be used during growth. The TEM and diffraction results average over large regions and also have not provided a quantitative measure of the composition.

In this Letter we report 1D confinement and a composition measurement of structures grown on vicinal substrates. These structures solve two serious problems of TSL preparation and characterization: The tilt is extremely sensitive to the per-cycle coverage; and the incomplete step-flow growth reduces the composition modulation. The tilt sensitivity is avoided by sweeping the per-cycle coverage through a range including that needed for a vertical structure, giving a "serpentine superlattice" (SSL) [21]. This can ensure a particular confinement geometry across a substrate despite systematic deposition

errors that make TSLs impractical. For (Al,Ga)As structures, too much AlAs and imperfect segregation can give an indirect heterostructure and thus no luminescence for characterization. A direct-gap structure is ensured by using lower-AlAs-content lateral barriers composed of alternating partial layers in the vertical direction: a "digital alloy."

Figure 1 displays a TEM micrograph from a SSL sample, with the lighter regions corresponding to higher Al content. At the turning points, the electronic states may be quasi-1D or 2D confined, depending on the lateral coupling. The important case is a linear sweep of the per-cycle coverage, giving parabolic arcs for the quantum-well boundaries defined by $\tan\beta = z/(z_0 \tan\alpha)$. Here β is the angle of the tangent of the arc with respect to the nearby major crystal axis and z is the growth direction coordinate. The change in coverage per thickness grown, $1/z_0$, is a well-controlled parameter in MBE. A systematic coverage error simply translates the parabola along z. The two dimensions of quantum confinement are determined by curvature, lateral step period, the fraction of each step covered by the barrier, and the height of the barrier. In the conduction band, E_{1D} is predicted to be 100 meV for ideal composition modulation [22].

The SSL of Fig. 1 was grown to have digital alloy $Al_{1/2}Ga_{1/2}As$ lateral barriers that cover $\frac{3}{7}$ terrace with $z_0 = 509$ nm, on a substrate nominally misoriented by $\alpha = 2°$. The lower crescents were to be formed by sweeping the coverage from 1.1 to 0.9 monolayer per cycle, and the upper crescents by sweeping back through this range. The micrographs indicate $\alpha = 1.94°$ from the lateral period, and an actual range of coverages from 1.15 to 0.95 monolayer per cycle [23]. Thus, even though a systematic error in the coverage of 5% is measured, the SSL displays the intended cross sections, shifted along z. In contrast, a TSL with this error would be tilted by over 50° [8].

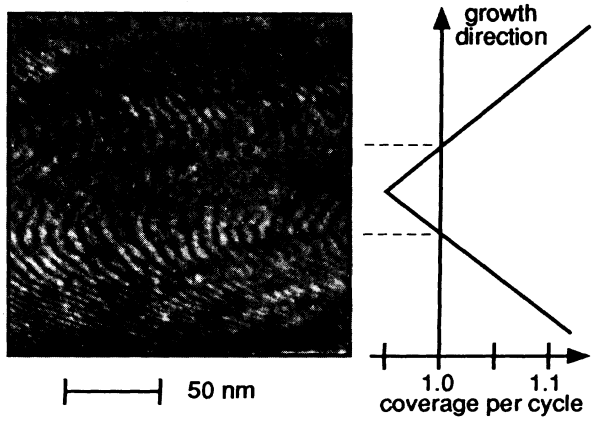

FIG. 1. A cross-section TEM micrograph of a SSL is displayed on the left, with the lighter regions corresponding to higher Al concentrations. On the right is shown the corresponding fractional coverage per cycle.

We present here polarization-dependent photoluminescence (PL) and PLE spectra, total lifetimes, and power dependences of spectral features taken at 1.4 K. More extensive results appear elsewhere [24]. Figure 2 gives PL spectra for a parabolic SSL having $Al_{1/3}Ga_{2/3}As$ digital alloy barriers covering $\frac{1}{2}$ step with $z_0 = 174$ nm and $\alpha = 2°$. The SSL arcs have been confirmed with TEM; they span 51.0 nm. The SSL is clad with $Al_{0.35}Ga_{0.65}As$ barriers that in turn contain 6.0- and 8.0-nm-wide quantum wells. A control sample was prepared on a (001) substrate, with the SSL replaced by a digital alloy of the same average composition. The pump laser intensity, in both the PL and PLE experiments, was close to 1 $W cm^{-2}$. The data were collected while observing along the z direction (see inset), with a polarizing Glan-Thompson prism analyzing the light, and have been corrected for the polarization dependence of the monochromator. Solid and dashed curves represent light polarized parallel and perpendicular to the quantum wires. The peak at 1.735 eV is assigned to the SSL and has a full width at half maximum (FWHM) of 7.0 meV. The SSL peak is shifted from that of the alloy control sample by 12 meV [24]. The polarization of the SSL peak, P_z, is defined in terms of the intensities of the light polarized in the x and y directions, I_x and I_y, as $P_z = (I_x - I_y)/(I_x + I_y) = 23\%$. Measuring the polarization of the light from cleaved {011} facets, we find $P_x = 36\%$ and $P_y = 57\%$, where indices are cyclically permuted. The polarizations for the 6 nm quantum well are $P_z = 0\%$, $P_x = 67\%$, and $P_y = 76\%$, consistent with reported values [25]. The GaAs buffer layer PL peak was unpolarized in all three directions, and the SSL control sample had $P_z = 0\%$. The lifetimes for the SSL and control sample peaks were 379 and 262 ps, respectively. In both the SSL and the control samples the lifetimes for the 8.0 and 6.0

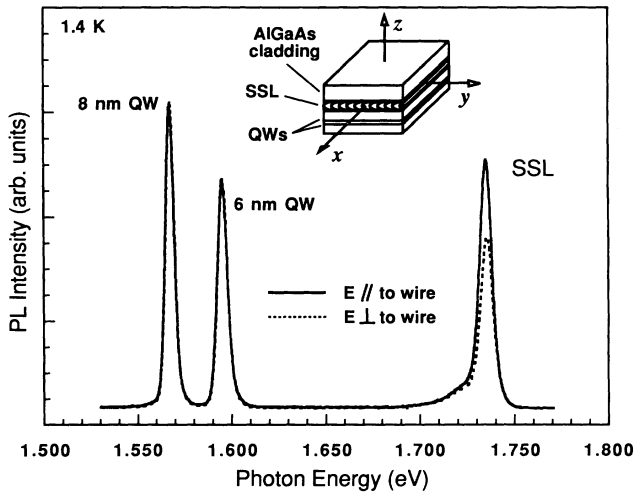

FIG. 2. The polarization-dependent PL spectra are given with the direction of observation, along the z axis here, defined in the inset.

nm quantum wells were 250 ± 10 ps. All these spectral features exhibited a linear intensity dependence on the power of the excitation over 3 orders of magnitude [24].

Figure 3 presents PLE data obtained by detecting the PL in the z direction at the low-energy side of the SSL peak. A Ti:sapphire laser polarized with a Glan-Thompson prism excited the specimen normal to the vicinal surface. The two PLE spectra are for the excitation polarized parallel and perpendicular to the wires, represented by the solid and dashed lines. Each spectrum shows a peak, Stokes shifted from the detection energy by 4.6 meV for parallel polarization and by 6.6 meV for perpendicular polarization, giving a 2.0-meV relative separation. Corresponding PLE spectra taken for the 6 nm quantum well and the alloy control do not show an anisotropy.

Using the envelope approximation, we have calculated conduction band states, four coupled valence band states, and the light polarization from conduction band to valence band transitions [22]. The imperfect lateral segregation is parametrized by considering AlAs to be uniformly removed from the barrier and uniformly redistributed into the well. Figure 4 gives P_z for heavy- and light-hole transitions. Notice that even for relatively weak segregation we expect to see significantly polarized light. The three polarizations should be largely determined, for a given segregation, by the aspect ratio of the quantum-wire cross section [26], and will be a distinctive signature of the confinement geometry.

Each polarization independently yields an estimate of the segregation. With $P_z = 23\%$ for the SSL, Fig. 4 indicates alloy compositions of $x_{\text{well}} = 0.14$ and $x_{\text{barrier}} = 0.19$. Similarly, P_x and P_y give $x_{\text{barrier}} = 0.21$ and 0.22. The three results are in good agreement and, on taking the average, indicate a value for the barrier alloy of $x_{\text{barrier}} = 0.21$. The SSL peak shift from that of the alloy control indicates $x_{\text{barrier}} = 0.24$. These correspond to a potential-energy difference V between the barrier and the well of some 80 meV in the conduction band. Our calculations show that the hole states are confined to 1D while the electron states are coupled through the lateral barriers because of the lighter effective mass and are confined to 2D. The linear intensity dependence of the SSL PL peak on the excitation power indicates monomolecular, excitonic recombination. The heterostructure is thus probed by luminescence on a scale of 10 nm by an exciton formed from 1D hole states and 2D electron states. The lifetime of the SSL exciton peak is longer than for the control sample, consistent with increased excitonic lifetimes reported for other 1D systems [27].

The 7.0 meV FWHM of the SSL PL peak is greater than the expected valence band subband splittings, obscuring these finer features. In spite of this, the PLE data *do* give evidence for confinement by the SSL. Figure 4 shows that for light polarized parallel or perpendicular to the wire, the lowest-lying heavy-hole (hh) or light-hole (lh) states will be resonantly excited, qualitatively consistent with the spectra of Fig. 3. If we estimate the $e1$hh-$e1$h splitting with the 2.0-meV shift, we infer effective alloy compositions of $x_{\text{well}} = 0.11$ and $x_{\text{barrier}} = 0.22$, in agreement with the PL estimates.

In summary, we have grown SSL samples that show the intended geometry. The optical characterizations show a distinct anisotropy and allow us to conclude, by fitting five measurements with a single value of one pa-

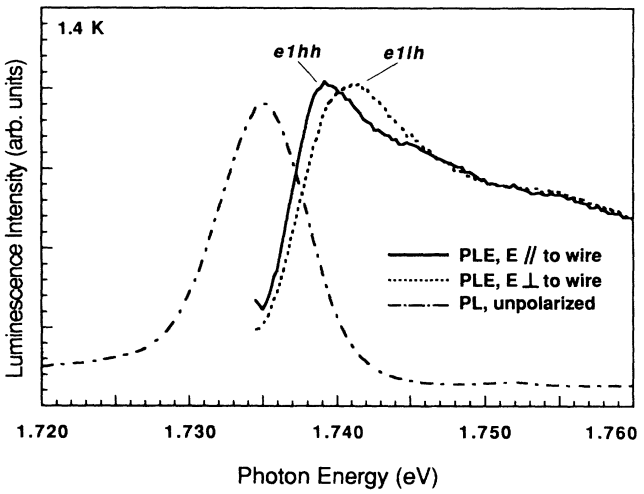

FIG. 3. The polarization-dependent PLE spectra for absorption in the z direction are given for the sample of Fig. 2. The solid and dashed lines are for the exciting light polarized parallel and perpendicular to the quantum wires, respectively, while the dash-dotted line is the unpolarized PL.

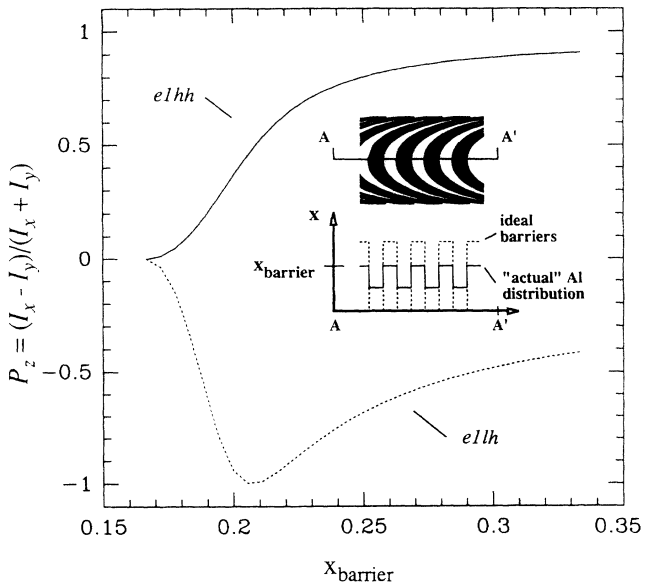

FIG. 4. The polarization of light in $e1$hh-like and $e1$lh-like transitions is plotted as a function of the Al content of the barrier, x_{barrier}. The Al distribution is defined in the inset.

rameter, that the hole states are confined to 1D with $E_{1D} \sim 2$ meV, and that 2D electron states are coupled through the lateral barriers. The lifetimes are longer for these low-dimensional heterostructures than for a corresponding alloy structure. Last, we have characterized the AlAs distribution from the SSL step-flow growth and found that one-third of the Al intended for the barrier instead incorporates in the well.

We gratefully acknowledge the support of the NSF, AFOSR, and ONR.

---

[a]Current address: Department of Physics, Linköping University, S-581 83, Lonköping, Sweden.

[1] D. A. Wharam, T. J. Thornton, R. Newbury, M. Pepper, H. Ahmed, J. E. F. Frost, D. G. Hasko, D. A. Ritchie, and G. A. C. Jones, J. Phys. C **21**, L209 (1988); M. Kohl, D. Heitmann, P. Grambow, and K. Ploog, Phys. Rev. Lett. **63**, 2124 (1989); Gregory L. Snider, Mark S. Miller, Michael J. Rooks, and Evelyn L. Hu, Appl. Phys. Lett. **59**, 2727 (1991).

[2] K. Kash, B. P. Van der Gaag, Derek D. Mahoney, A. S. Gozdz, L. T. Florez, and J. P. Harbison, Phys. Rev. Lett. **67**, 1326 (1991).

[3] E. Kapon, D. M. Hwang, and R. Bhat, Phys. Rev. Lett. **63**, 430 (1989).

[4] R. J. Haug, H. Munekata, and L. L. Chang, Surf. Sci. **263**, 374 (1992).

[5] H. L. Stormer, L. N. Pfeiffer, K. W. Baldwin, K. W. West, and J. Spector, Appl. Phys. Lett. **58**, 726 (1991).

[6] R. Nötzel, N. N. Ledentsov, L. Däweritz, M. Hohenstein, and K. Ploog, Phys. Rev. Lett. **67**, 3812 (1991).

[7] P. M. Petroff, A. C. Gossard, and W. Wiegman, Appl. Phys. Lett. **45**, 620 (1984).

[8] J. M. Gaines, P. M. Petroff, H. Kroemer, R. J. Simes, R. S. Geels, and J. H. English, J. Vac. Sci. Technol. B **6**, 1378 (1988).

[9] S. A. Chalmers, H. Kroemer, and A. C. Gossard, Appl. Phys. Lett. **57**, 1751 (1990).

[10] Takashi Fukui and Hisao Saito, J. Vac. Sci. Technol. B **6**, 1373 (1988).

[11] M. Tsuchiya, J. M. Gaines, R. H. Yan, R. J. Simes, P. O. Holtz, L. A. Coldren, and P. M. Petroff, Phys. Rev. Lett. **62**, 466 (1989).

[12] D. S. Citrin and Yia-Chung Chang, J. Appl. Phys. **70**, 867 (1991).

[13] H. Weman, M. S. Miller, and J. L. Merz (to be published).

[14] Masaaki Tanaka and Hiroyuki Sakaki, Appl. Phys. Lett. **54**, 1326 (1989).

[15] E. W. Bauer and Hiroyuki Sakaki, Phys. Rev. B **44**, 5562 (1991).

[16] Masaaki Tanaka, Takashi Suzuki, and Tatau Nishinaga, Jpn. J. Appl. Phys. **29**, L706 (1990); G. L. Kellogg and A. F. Voter, Phys. Rev. Lett. **67**, 622 (1991); Eric Ganz, Silva K. Theiss, Ing-Shouh Hwang, and Jene Golovchenko, Phys. Rev. Lett. **68**, 1567 (1992).

[17] Dietrich E. Wolf, Phys. Rev. Lett. **67**, 1783 (1991); Makio Uwaha and Yukio Saito, Phys. Rev. Lett. **68**, 224 (1992).

[18] Dimitri Vvedensky and Shaun Clarke, Surf. Sci. **225**, 373 (1990); Andrea K. Myers-Beaghton and Dimitri D. Vvedensky, Phys. Rev. B **42**, 9720 (1990).

[19] J. H. Neave, P. J. Dobson, B. A. Joyce, and J. Zhang, Appl. Phys. Lett. **47**, 100 (1983); P. R. Pukite, J. M. Van Hove, and P. I. Cohen, J. Vac. Sci. Technol. B **2**, 243 (1984).

[20] M. D. Pashley, K. W. Haberern, and J. M. Gaines, Appl. Phys. Lett. **58**, 406 (1991).

[21] M. S. Miller, C. E. Pryor, H. Weman, L. A. Samoska, H. Kroemer, P. M. Petroff, and J. L. Merz, J. Cryst. Growth **111**, 323 (1991).

[22] Craig Pryor, Phys. Rev. B **44**, 12912 (1991).

[23] M. Krishnamurthy, M. S. Miller, and P. M. Petroff (to be published).

[24] H. Weman, M. S. Miller, C. E. Pryor, M. Krishnamurthy, P. M. Petroff, and J. L. Merz (to be published).

[25] J. S. Weiner, D. S. Chemla, D. A. B. Miller, H. A. Haus, A. C. Gossard, W. Wiegman, and C. A. Burrus, Appl. Phys. Lett. **47**, 664 (1985).

[26] C. McIntyre and L. Sham, Phys. Rev. B **45**, 9443 (1992).

[27] R. Cingolani, H. Lage, L. Tapfer, H. Kalt, D. Heitmann, and K. Ploog, Phys. Rev. Lett. **67**, 891 (1991).

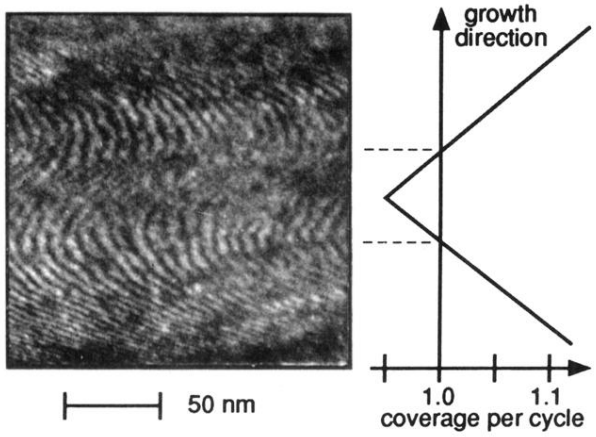

FIG. 1. A cross-section TEM micrograph of a SSL is displayed on the left, with the lighter regions corresponding to higher Al concentrations. On the right is shown the corresponding fractional coverage per cycle.

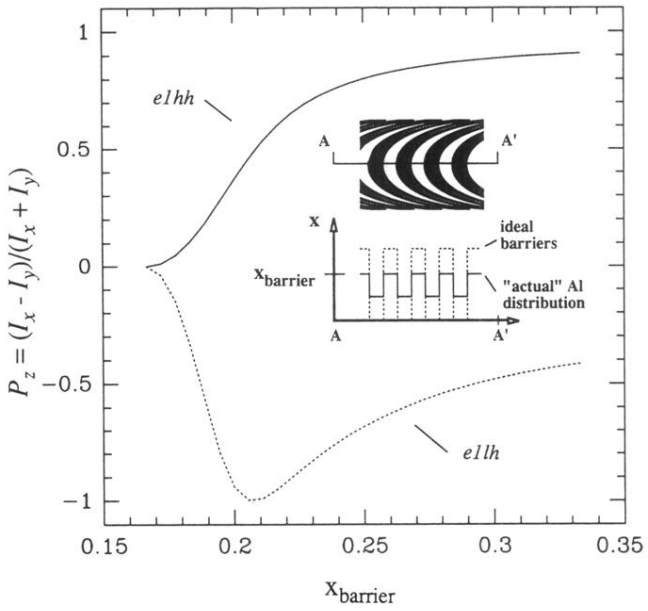

FIG. 4. The polarization of light in $e1$hh-like and $e1$lh-like transitions is plotted as a function of the Al content of the barrier, x_{barrier}. The Al distribution is defined in the inset.